WP 2013-11
February 2013

Working Paper

Charles H. Dyson School of Applied Economics and Management
Cornell University, Ithaca, New York 14853-7801 USA

AN AGENT-BASED COMPUTATIONAL BIOECONOMIC MODEL OF PLANT DISEASE DIFFUSION AND CONTROL: GRAPEVINE LEAFROLL DISEASE

Shady Atallah, Miguel Gómez, Jon Conrad and Jan Nyrop

It is the Policy of Cornell University actively to support equality of educational and employment opportunity. No person shall be denied admission to any educational program or activity or be denied employment on the basis of any legally prohibited discrimination involving, but not limited to, such factors as race, color, creed, religion, national or ethnic origin, sex, age or handicap. The University is committed to the maintenance of affirmative action programs which will assure the continuation of such equality of opportunity.

An Agent-Based Computational Bioeconomic Model of Plant Disease Diffusion and Control: Grapevine Leafroll Disease

Shady S. Atallah*
Charles H. Dyson School of Applied Economics and Management
Cornell University
302B Rice Hall
Ithaca, NY 14853
Phone: 916-601-2207
Fax: 607-255-9984
E-mail: sa589@cornell.edu

Miguel I. Gómez
Charles H. Dyson School of Applied Economics and Management
Cornell University
321 Warren Hall
Ithaca, NY 14853
Phone: 607-255-8159
E-mail: mig7@cornell.edu

Jon M. Conrad
Charles H. Dyson School of Applied Economics and Management
Cornell University
431 Warren Hall
Ithaca, NY 14853
Phone: 607-255-7681
E-mail: jmc16@cornell.edu

Jan P. Nyrop
Department of Entomology
New York State Agricultural Experiment Station
Geneva, NY 14456
Phone: 315-787-2355
E-mail: jpn2@cornell.edu

February, 2013

* Corresponding author

An Agent-Based Computational Bioeconomic Model of Plant Disease Diffusion and Control: Grapevine Leafroll Disease

Abstract

Grapevine leafroll disease threatens grape harvests in the United States and around the world. This viral disease reduces yield, delays fruit ripening, and affects wine quality. Its spatial-dynamic diffusion process remains poorly understood and little is known about profit-maximizing control strategies. In this article, we model the disease spatial-dynamic diffusion in a vineyard, evaluate nonspatial and spatial control strategies, and rank them based on expected net present values. Nonspatial strategies consist of roguing and replacing symptomatic grapevines with and without considering vine age. In spatial strategies, symptomatic vines are rogued and replaced, and their nonsymptomatic neighbors are virus-tested, then rogued and replaced if the test is positive. We find that age-structured strategies outperform their nonage-structured counterparts. More importantly, we show that spatial strategies dominate nonspatial strategies, increasing the vineyard expected net present value by 40 percent relative to the baseline of no control.

Key words: Agent-based Computational Economics, Agriculture, Bioeconomic Models, Disease Control, Grapevine Leafroll Disease, Spatial-Dynamic Processes

JEL Codes: C15, C63, D24, Q12

Grapevine leafroll disease (GLRD) presently threatens grape harvests in the United States (Fuchs et al. 2009; Golino et al. 2008; Martin et al. 2005) and around the world (Cabaleiro et al. 2008; Charles et al. 2009; Martelli and Boudon-Padieu 2006). This viral disease reduces yield, delays fruit ripening, and affects wine quality by lowering soluble solids and increasing fruit juice acidity (Goheen and Cook 1959; Martinson et al. 2008). Its economic impact was recently estimated at $25,000- $40,000 per hectare over a 25 year-period in New York State vineyards if the disease is left uncontrolled (Atallah et al. 2012). GLRD is primarily transmitted via vegetative propagation. However, there is increasing evidence that, once introduced through infected planting material, the disease is transmitted to healthy vines by several species of mealybugs (Hemiptera: Pseudococcidae) and soft-scale insects (Hemiptera: Coccidae) (Martelli and Boudon-Padieu 2006; Pietersen 2006; Tsai et al. 2010). Recent plant pathology studies have examined the spatiotemporal insect-facilitated diffusion patterns of the disease (Cabaleiro et al. 2008; Jooste et al. 2011). However, the spatial dynamics of the disease spread process remains poorly understood and profit-maximizing strategies to control disease diffusion are unclear.

Multiple disciplines have taken complementary approaches when modeling disease diffusion and control, including ecology, economics and epidemiology. Generally, this literature employs aggregate models (often referred to as top-down models) that make simplifying assumptions in order to ensure mathematical tractability. These assumptions include perfect population mixing and homogeneity of the agents under study. They are too restrictive, particularly for decision-makers who might want to develop disease intervention programs targeting specific heterogeneous agents based on their role in disease transmission (Greenhalgh 2011). More recently, with dramatic decreases in computational costs, agent-based modeling (ABM) has emerged as a tractable theoretical and experimental framework to study complex

adaptive systems (Miller and Page 2007). Disease diffusion systems can be treated as complex adaptive systems because they are composed of adaptive agents whose local interactions produce outcomes that cannot be wholly explained by breaking down the system into its individual parts (Miller and Page 2007; Teose et al. 2011).The bottom-up approach of ABMs allows the analyst to account for complex interactions between heterogeneous agents. However, a primary disadvantage is that the relatively easier model construction and validation of top-down aggregate models is lost (Osgood 2007). ABMs are also harder to parameterize and validate (Rahmandad and Sterman 2008). When used in epidemiological research, these two modeling paradigms have yielded results that are consistent in some cases (e.g. Schneckenreither et al 2008), while divergent in their public policy implications in other cases (e.g. Rahmandad and Sterman 2008).

This paper develops an agent-based computational bioeconomic model of disease diffusion and control to identify profit-maximizing strategies for GLRD diffusion control. The model allows for a full spatial-dynamic characterization of the disease diffusion. It relaxes the assumptions of homogeneity and perfect mixing. Instead, in the model, the choice of disease control strategy takes into account agent heterogeneity in location, virus detectability, age, own infection state, and infection states of vines in the neighborhood. We examine the impact of alternative disease control strategies on a distribution of bioeconomic outcomes and rank them based on the vineyard expected net present values they yield. We find that profit-maximizing strategies reflect important ecological and economic tradeoffs in the location, timing, and intensity of disease control. The results highlight the potential of novel, vine-level, spatial strategies in reducing the economic impacts of GLRD under imperfect information. In addition, our results can be generalized to address disease diffusion and control issues in other perennial

crops. We are not aware of previous work in agricultural and resource economics or agent-based computational economics that formulates an agent-based model of plant disease diffusion and control.

Literature Review

The unique characteristics of certain insect-transmitted plant diseases condition the choice of modeling approaches. In general, such diseases are controlled by reducing the population of disease vectors and minimizing secondary sources of infection by roguing (removing) infected plants and replacing them with healthy ones (Chan and Jeger 1994). In the case of GLRD, however, insect vectors can have a short infectivity retention period [1] and can spread disease rapidly, even if their population is kept at a low density (Tsai et al. 2008). This transmission characteristic renders vector control methods ineffective in the case of GLRD (Cabaleiro and Segura 2006, 2007) and limits the applicability of existing pest and damage control models (Babcock, Lichtenberg, and Zilberman 1992; Saphores 2000).

Plant heterogeneity is the second characteristic of many diseases and suggests the need to develop plant-level models for optimal GLRD disease control. Specifically, individual vines that are infected but nonsymptomatic are heterogeneous in the time it takes for their virus population to be detectable (Cabaleiro and Segura 2007; Constable et al. 2012). An additional relevant plant-level characteristic results from the age-dependency in the latency period of the disease. In the case of GLRD, this latency period is decreasing with age causing younger vines to transition from the latent to the infective states faster than older ones (Pietersen 2006).

A third characteristic of plant diseases is that they are simultaneously driven by integrated dynamic and spatial forces, rather than by dynamic processes alone. When diseased

plants are heterogeneously distributed in space and the physical environment includes spatial constraints on disease diffusion, the efficiency of disease control is affected by its location, timing, and intensity. Therefore, effective control has to simultaneously consider the spatial gradient of disease diffusion and the spatial gradient of revenues. Taken together, these three characteristics call for plant-level, spatial-dynamic models of disease diffusion and control.

Aggregate Bioeconomic Models

Research on the economics of agricultural disease control has increasingly moved away from pest threshold models (Hall and Norgaard 1973 and towards integrated epidemiological models (Beach et al. 2007; Fenichel and Horan 2007; Horan and Wolf 2005) that incorporate feedbacks between economic and disease diffusion components within the model. These models typically aggregate individuals into disease-state (e.g. Horan et al. 2010) or age-state (e.g. Tahvonen 2010) compartments, and employ differential or difference equations (DEs) to represent transition between states. However, DEs assume within-compartment homogeneity and population perfect mixing (Brauer and Castillo-Chavez 2001). These assumptions are limiting in disease modeling, especially in the case of GLRD where (1) plants are heterogeneous in disease detectability, (2) population age-structure is critical to disease transmission, and (3) disease diffusion follows imperfect mixing processes (Pietersen 2006; Constable et al. 2012). The homogeneity assumption of aggregate models is particularly restrictive because it precludes the formulation and testing of disease control strategies targeting agents based on their heterogeneous, spatial-dynamic attributes. These assumptions can be relaxed to represent distinct groups exhibiting preferential mixing or other important characteristics by increasing the number of subpopulations or dividing the subpopulations into smaller stocks (e.g. Medlock and Galvani 2009). This process, however, leads to an explosion in the number of state variables, equations, parameters,

and data requirements (Teose et al. 2011). Moreover, in aggregate bioeconomic models, disease transmission rates are imposed on agents exogenously in a top-down fashion depending on membership in a specific subpopulation. In reality, however, transmission rates are endogenously determined in a spatial-dynamic, bottom-up fashion as a result of local agent interaction and disease control strategies.

Spatial Bioeconomic Models

Spatial-dynamic processes have only recently been studied by economists and the bioeconomic literature on agricultural diseases and invasive species control is mostly nonspatial (Wilen 2007). Sanchirico and Wilen (1999, 2005) show that ignoring the spatial revenue gradient can lead to suboptimal managerial decisions. Space can be incorporated in bioeconomic disease models by specifying location-dependent, state-transition probabilities (e.g., Karl and Winter-Nelson 2007), or by using partial differential equations (Holmes et al. 1994). In such models, spatial heterogeneity is exogenous and fixed over time (see review in Smith, Sanchirico and Wilen 2009). In reality, however, spatial heterogeneity can be endogenously determined by the diffusion process, and dynamically affected by the implementation of control strategies. The challenge of incorporating spatial feedbacks into state dynamics is a common thread in resource economics and not confined to disease dynamic models (Smith, Sanchirico and Wilen 2009). Moreover, spatial bioeconomic models often make restrictive assumptions such as linear growth and control to achieve tractability or to focus on steady state analysis in simple landscapes (see review in Epanchin-Niell and Wilen 2012). Relaxing such assumptions, however, precludes analytical solutions and calls for numerical methods in most applications (Wilen 2007; Smith, Sanchirico and Wilen 2005).

Agent-Based Models

In contrast to aggregate models, agent-based models (ABMs), also called individual-based models (IBMs) in the ecology literature (Railsback and Grimm 2012), allow the study of a population of heterogeneous agents living in a spatial-dynamic world. These are computationally intensive simulation models where agents interact with their environment and each other according to rule-based algorithms and mathematical equations (Tesfatsion 2006). Agent interaction gives rise to a distribution of system-wide nonlinear outcomes which cannot usually be deduced from the rules faced by agents. ABMs are appropriate in high-resolution settings because they represent spatial agents with complex characteristics and they capture the interactive properties of natural and human systems as well as the complex outcomes that emerge from their interaction (White and Engelen 2000). They are also appealing because they offer a balance between flexibility (ability to capture a wide class of agent behavior) and precision (exact definition of model elements). Further, ABMs are inherently dynamic, scalable (number of agents), fully observable, and repeatable (table 1).

The agent-based computational economics (ACE) literature has explored feedbacks between social and ecological systems with applications in fishery economics (e.g. BenDor, Scheffran, and Hannon 2009), industrial organization (e.g. Sun and Tesfatsion 2007), production economics (e.g. Akanle and Zhang 2008) and policy analysis (e.g. Rahimiyan and Mashhadi 2010). Applications in agricultural economics are, however, less common (Berger 2001), and we are unaware of research using ABMs to model the bioeconomics of agricultural disease diffusion and control. Agent-based modeling is an appropriate framework to simulate the spatial-dynamic diffusion of an agricultural disease in a heterogeneous population and generate distributions of bioeconomic outcomes under alternative disease control strategies. Outputs can then be

statistically analyzed to evaluate policy implications (Fagiolo, Birchenhall and Windrum 2007). This modeling approach is well suited to model the diffusion of GLRD in a vineyard, because vines are heterogeneous in their location and dynamic attributes (age and infection states), and because a vine's neighborhood state is endogenously determined by the disease diffusion process and the control strategies employed. In addition, multilevel heterogeneity can be exploited to devise and test novel disease control strategies.

Applying agent-based computational economic models to agricultural disease management is timely because of the recent technological advancement in and adoption of precision agriculture. Precision agricultural technology, with its focus on management according to spatial variability, is relevant in agricultural systems where high within-farm variation in environmental factors affects the growth of individual plants (Hall et al. 2008). Precision viticulture applications to GLRD management include spectral reflectance[2], a promising profit-maximizing and nondestructive disease detection and control tool based on visual symptoms of individual vines (Naidu et al. 2009).

We contribute to the disease control bioeconomic literature by employing the modeling principles of agent-based computational economics and individual-based ecology to characterize a problem of agricultural disease diffusion and control. Using a cellular automaton, we offer a model that is inherently spatial and dynamic. We allow agents to be heterogeneous in their location and dynamic attributes and allow them to interact in a dynamic environment whose geometry and boundaries are explicitly defined. Disease is initialized following a random spatial distribution and stochastic agent interactions gives rise to disease diffusion. We generate distributions of bioeconomic outcomes for the baseline case of no control and under alternative disease control strategies.

Disease Diffusion Model

We develop a stochastic agent-based model of disease diffusion and control that is discrete in both time and space. The model is spatially explicit and the population consists of agents that are heterogeneous in their location, age and infection states.

Agents

Plant viral diseases are systemic, meaning that the whole plant is infected, rendering it a suitable modeling unit (Chan and Jeger 1994). In our model, an agent is a grapevine. Agents are characterized by their *states* and relevant dynamic *processes*. They are endowed with static states, namely locations that define their local neighborhoods. Agents also have two dynamic states: age and infection. Agents are heterogeneous in age and infection states, as well as the age-dependency of the infection latency period. The latter is defined as the interval of time after a vine gets infected and before it becomes infective. An agent's infection and age states map into a third dynamic state variable: the agent's economic value. Agents use *processes*, such as rule-based algorithms, to perceive their environment (including agents in their neighborhood) and to send messages to other agents (Macal and North, 2010). In our model, one *process* gives infective agents the ability to perceive the location and infection status of neighboring vines and to send them a message according to certain rules. In each period, the message is sent by infective agents to their healthy within-column neighbors with a higher probability than it is to their across-column healthy neighbors. Once received by a healthy agent, a message triggers the agent's transition to an infected state. We choose this neighborhood-based infection state transition process to reflect patterns of GLRD diffusion observed in spatial analyses where the disease is shown to spread preferentially along columns (Habili et al. 1995; Le Maguet et al. 2012).

Agent environment: cellular automaton

A cellular automaton is a dynamic model that operates in discrete space and time on a uniform and regular lattice of cells. Each cell is in one of a finite number of states that get updated according to mathematical functions and algorithms that constitute state transition rules. At each time step, a cell computes its new state given its old state and the states of its neighborhood according to the transition rules (Tesfatsion 2006; Wolfram 1986). When used in agent-based models, a cellular automaton provides agents with a rule-based, spatial-dynamic structure capable of modeling complex behavior based on simple, local state transition rules (White and Engelen 2000). The spatial-dynamic structure is especially relevant when the physical environment includes constraints on the agent's spatial interaction, such as boundaries and geometry (Gilbert and Terna, 2000). Combining a cellular automaton with an agent-based model provides an adequate spatial-dynamic environment to simulate GLRD diffusion: the vineyard is represented by a grid where cells are occupied by agents (the grapevines) whose infection and age states, locations and interactions determine disease diffusion. In what follows, we describe the elements of the cellular automaton and the features of the agent-based model that integrates them: the cells and their states, the cell neighborhoods, and their states, the cell transition rules, and the time step.

The cell and its state $W_{i,j}^{t}$

Cells are the units that make up the two-dimensional rectangular grid. The grid defines the spatial geometry and represents a vineyard plot with (I x J) cells where I and J are the number of rows and columns, respectively. In our model, there are 5,720 cells each holding only one agent representing a grapevine. Vineyard rows are oriented north to south with I=44 vines per row and J=130 vines per column. This configuration is considered representative of a typical vineyard in

the Northeastern United States[3] (Wolf 2008). Each cell holds only one composite state in any period. The state of a cell located in row *i* and column *j* at time *t+1* ($W_{i,j}^{t+1}$) can be represented as a function *f* of the cellular automaton's elements at time *t* as follows (Ozah et al 2010):

(1) $$W_{i,j}^{t+1} = f(W_{i,j}^{t}, S_{N_{i,j,k}}^{t}, R_{i,j}, \Delta t)$$

where $W_{i,j}^{t}$ is the age-infection state of cell (*i* ,*j*) at time *t* ; $S_{N_{i,j,k}}^{t}$ is the state of cell (*i*,*j*)'s neighborhood $N_{i,j}^{t}$ that is of type *k* at time *t*; $R_{i,j}$ is the state transition rule; and Δt the time step.

$W_{i,j}^{t}$ is an age-infection composite state defined as the combination of a vine's age state $A_{i,j}^{t}$ and a vine's infection state $S_{i,j}^{t}$. The infection state space $S_{i,j}^{t}$ of a vine located at cell (*i, j*) is $\{H, E_d, E_u, I_m, I_h\}$. *H* is the *Healthy* state that describes vines that are susceptible to infection. *E* is the *Exposed* or latent infection state, during which a vine is infected, nonsymptomatic, and not yet infective. *E* is a composite state made of two simple states: *Exposed-undetectable* and *Exposed-detectable*. The distinction between those two states is important given that GLRD does not reach detectable levels until a certain period after inoculation. I_m (*Infective-moderate*) and I_h (*Infective-high*) represent the states of infective grapevines with moderate and high disease symptom severity, respectively. We refer to states *H* and *E* collectively as the composite state *NI* (*Noninfective*) in which a grapevine in noninfective. Similarly, we refer to states I_m and I_h collectively as the composite state *I* (*Infective*) that denotes vines that have the ability to transmit the infection. The age state space of a vine, $A_{i,j}^{t}$, is $\{1, 2, \ldots, A_{max}\}$. Combining the infection and age states into a space of composite age-infection states $W_{i,j}^{t}$ allows modeling the fact that (1) younger vines have shorter latency periods (Pietersen 2006), i.e. they transition from *E* to I_m faster than older vines; and (2) a vine's economic value increases with the age state transition but decreases with the infection state transition. As a vine goes through the five infection states, its economic value decreases as its yield and grape juice quality are reduced. The age state acts in

the opposite direction: a vine is unproductive for three year after planting. Then, its economic value increases as it ages. We discretize the age space into *Young* (0 to 5 years), *Mature* (5-20 years) and *Old* (20 years and above) age categories. We do so to allow the transition out of latency to be dependent on the vine age category. We also use these age categories to formulate age-structured disease control strategies.

The cell neighborhood $N_{i,j}^t$ and its state $S_{N_{i,j,k}}^t$

Charles et al. (2009) observed that once GLRD is introduced through unsanitary vines at planting, leafroll-associated viruses are then transmitted through mealybugs which have limited mobility within columns through dispersal of infected mealybug crawlers. The virus is transmitted between columns, although to a lesser extent, either through human-assisted movement of mealybug crawlers or through aerial dispersal of infective mealybugs (Cabaleiro et al. 2008; Jooste et al. 2011).

Given the limited mobility of the grapevine leafroll disease vectors, we give the agents a von Neumann neighborhood type in which each agent has four neighbors in the four cardinal directions (north, south, east, west) (figure 1). This neighborhood type allows defining infection-state transition rules that are different for within-column (i.e., north and south) and across-columns (i.e., east and west) disease transmission. This allows us to model the observed preferential within-column spread of the disease (Habili et al 1995; Le Maguet et al 2012). For a vine $V_{i,j}$ located in cell (i, j), the neighborhood $N_{i,j}^t$ can be expressed as:

(2) $$N_{i,j}^t = \{ V_{i,j-1}, V_{i,j+1}, V_{i-1,j}, V_{i+1,j} \}$$

$$(j-1) \in \{1, J-1\}; (j+1) \in \{1, J-1\}; (i-1) \in \{1, I-1\}; (i+1) \in \{2, I\}$$

where the first two elements represent across-column neighbors to the west and to the east and the last two elements represent within-column neighbors to the north and south of vine $V_{i,j}$. The

intervals on the indices of vine (*i*, *j*)'s neighbors define the spatial boundary conditions on disease diffusion.

[Insert figure 1 here]

The infectivity state of cell *(i,j)* 's neighborhood at time t ($S^t_{N_{i,j,k}}$ in Equation 1) is determined by the individual infectivity (*Infective* and *Noninfective*) states ($S^t_{i-1,j}$ $S^t_{i+1,j}$, $S^t_{i,j-1}$, $S^t_{i,j+1}$) of the four neighboring cells *(i-1, j), (i+1, j), (i,j-1),* and *(i, j+1),* respectively. $S^t_{N_{i,j,k}}$ is therefore not fixed over time and is endogenously determined by disease diffusion and control strategies (e.g., roguing infected vines and replacing them with new, healthy ones). Given two possible infectivity states and four neighbors, $S^t_{N_{i,j,k}}$ can be one of 2^4 possible neighborhood infectivity states where $k \in \{1, 2, ..., 16\}$:

(3) $$S^t_{N_{i,j,k}} \in \{ S^t_{N_{i,j,1}} = (I, I, I, I), S^t_{N_{i,j,2}} = (I, I, I, NI), ..., S^t_{N_{i,j,16}} = (NI, NI, NI, NI)\}$$

Cell transition rules

The cell transition rules ($R_{i,j}$ in Equation 1) control the transitions within each of the age and infection state spaces. Given that age transitions are deterministic, we focus on the stochastic infection state transitions affecting the spatial-dynamic diffusion of the disease. We describe the stochastic initialization of the states; the stochastic neighborhood-dependent infection state transitions from *Healthy* to *Exposed-undetectable* [4]; the stochastic infection state transition within the *Exposed* (E_u to E_d) state; the stochastic age-dependent infection state transitions from *Exposed* to *Infective*; and the stochastic transition within the *Infective* state (I_m to I_h). We finally represent the infection transition rules in a Markov chain model.

Model Initial States

At the beginning of a simulation, two percent of the agents, homogeneous in their age-infection states ($S^t_{i,j} = H$ and $A^t_{i,j} = 0$), are chosen at random from a uniform distribution U (0, 5720) to

transition from *Healthy* to *Exposed*. This reflects findings in GLRD studies indicating that primary infection sources are randomly spatially distributed (Cabaleiro et al. 2008), and that initial disease prevalence is typically between 1 and 5 percent (Gómez et al 2010). Thereafter, GLRD spreads to uninfected vines according to rules that govern state transitions from *Healthy* to *Exposed*.

Stochastic neighborhood-dependent Healthy (H) to Exposed-undetectable (E_u) state transition

An infective vine transmits the virus to a neighboring healthy vine with a location-specific transmission rate. Following Constable et al. (2012), GLRD has a within-column preferential spread. We model this finding by letting infective vines transmit the disease to their within-column neighbors at a higher rate than they transmit it to their across-column neighbors. The continuous-time transmission rates are assumed to follow a Poisson process. That is, the waiting time X that it takes for a vine in the *Healthy* state to transition to the *Exposed-undetectable* state has an exponential distribution with parameter α for within-column transmission ($X_1 \sim \alpha e^{-\alpha X_1}$) and β for across-column transmission ($X_2 \sim \beta e^{-\beta X_2}$) with $0<\beta<\alpha$. Let B be the *Healthy* to *Exposed-undetectable* vector of transition probabilities conditional on previous own and neighborhood infection states. Mathematically, it can be expressed as

(4) $$B = \begin{pmatrix} \Pr(S_{i,j}^{t+1} = E \mid S_{i,j}^{t} = H,\ S_{N_{i,j,k}}^{t} = S_{N_{i,j,1}}^{t}) \\ \Pr(S_{i,j}^{t+1} = E \mid S_{i,j}^{t} = H,\ S_{N_{i,j,k}}^{t} = S_{N_{i,j,2}}^{t}) \\ \Pr(S_{i,j}^{t+1} = E \mid S_{i,j}^{t} = H,\ S_{N_{i,j,k}}^{t} = S_{N_{i,j,3}}^{t}) \\ \Pr(S_{i,j}^{t+1} = E \mid S_{i,j}^{t} = H,\ S_{N_{i,j,k}}^{t} = S_{N_{i,j,4}}^{t}) \\ \vdots \\ \Pr(S_{i,j}^{t+1} = E \mid S_{i,j}^{t} = H,\ S_{N_{i,j,k}}^{t} = S_{N_{i,j,13}}^{t}) \\ \Pr(S_{i,j}^{t+1} = E \mid S_{i,j}^{t} = H,\ S_{N_{i,j,k}}^{t} = S_{N_{i,j,14}}^{t}) \\ \Pr(S_{i,j}^{t+1} = E \mid S_{i,j}^{t} = H,\ S_{N_{i,j,k}}^{t} = S_{N_{i,j,15}}^{t}) \\ \Pr(S_{i,j}^{t+1} = E \mid S_{i,j}^{t} = H,\ S_{N_{i,j,k}}^{t} = S_{N_{i,j,16}}^{t}) \end{pmatrix} = \begin{pmatrix} 1 - e^{-(2\alpha+2\beta)} \\ 1 - e^{-(2\alpha+\beta)} \\ 1 - e^{-(2\alpha+\beta)} \\ 1 - e^{-2\alpha} \\ 1 - e^{-(\alpha+2\beta)} \\ 1 - e^{-(\alpha+\beta)} \\ 1 - e^{-(\alpha+\beta)} \\ 1 - e^{-\alpha} \\ 1 - e^{-(\alpha+2\beta)} \\ 1 - e^{-(\alpha+\beta)} \\ 1 - e^{-(\alpha+\beta)} \\ 1 - e^{-\alpha} \\ 1 - e^{-2\beta} \\ 1 - e^{-\beta} \\ 1 - e^{-\beta} \\ 0 \end{pmatrix}$$

where there are 2^4 possible neighborhood infectivity states, but only nine distinct conditional probabilities.[5] The *Healthy* to *Exposed-undetectable* state transition probabilities are triggered in each time step by a random variable u_t. Where u_t is a random draw from $U\sim(0, 1)$, the disease is transmitted from one infective vine to another healthy vine in the same column at time $t+1$ if $u_t < \alpha$. Conversely, the disease is not transmitted if $u_t \geq \alpha$. Similarly, the disease is transmitted from one infective vine to another healthy vine in an adjacent column at time $t+1$ if $u_t < \beta$ and is not transmitted if $u_t \geq \beta$.

Stochastic Exposed-undetectable (E_u) to Exposed-detectable (E_d) state transition

Before an infected grapevine develops visual symptoms, it is possible to reveal its infection state using virus testing techniques such as enzyme-linked immunosorbent assay (ELISA) or reverse transcription polymerase chain reaction (RT-PCR). The virus might, however, be below detectable levels until a year after infection, causing a risk of false-negative results. Cabaleiro and Segura (2007) and Constable et al. (2012) show that vines are heterogeneous in the time it takes their virus population to be high enough to test positive after infection. Those studies report a minimum, maximum and most common value for the period in which a vine is infected but

undetectable. With no further knowledge on the distribution of this period, we model it as a random variable drawn from a triangular distribution with parameters *a* (minimum), *b* (maximum), and *m* (mode). Then, where X_3 is the period it takes a vine to transition from E_u to E_d, the probability that the transition happens in less than *x* time units, or Pr ($X_3 < x$), is $\frac{(x-a)^2}{(b-a)(m-a)}$ for a $\leq x \leq m$. The probability is equal to 0 for $x < a$, $(1 - \frac{(b-x)^2}{(b-a)(m-a)})$ for $m \leq x < b$, and 1 for $x > b$ (Kotz and Rene van Dorp 2004).

Stochastic age-dependent Exposed-detectable (Ed) to Infective-moderate (Im) state transition

In order to account for shorter latency periods in younger vines, we let the latency period vary for the three age categories considered. We assume that the latency periods for young (L_y), mature (L_m) and old (L_o) vines follow exponential distributions with fixed rate parameters λ_y, λ_m, λ_o: $L_y \sim \text{Exp}(\lambda_y)$, $L_m \sim \text{Exp}(\lambda_m)$, $L_o \sim \text{Exp}(\lambda_o)$ where $\lambda_y < \lambda_m < \lambda_o$. The *Exposed-detectable* to *Infective* state transition probabilities conditional on age category can be represented mathematically in the vector *C* where:

$$C = \begin{pmatrix} \Pr\left(S_{i,j}^{t+1} = I_m \,\middle|\, S_{i,j}^{t} = E,\ A_{i,j}^{t} = Young\right) \\ \Pr\left(S_{i,j}^{t+1} = I_m \,\middle|\, S_{i,j}^{t} = E,\ A_{i,j}^{t} = Mature\right) \\ \Pr\left(S_{i,j}^{t+1} = I_m \,\middle|\, S_{i,j}^{t} = E,\ A_{i,j}^{t} = Old\right) \end{pmatrix} = \begin{pmatrix} 1 - e^{-\lambda_y} \\ 1 - e^{-\lambda_m} \\ 1 - e^{-\lambda_o} \end{pmatrix} \quad (5)$$

Stochastic transition from Infective-moderate (I_m) to Infective-high (I_h)

Once a vine is infected at the moderate level, symptom severity increases over time and reaches a high level after a fixed amount of time, denoted by *Inf*. The period that a vine spends in state I_m before it transitions to state I_h is exponentially distributed with fixed rate parameter φ: $Inf \sim \text{Exp}(\varphi)$. Thus, the probability that a vine transitions from I_m to I_h in one time step is defined as $\Pr(Inf<1) = 1 - e^{-\varphi}$, or $\Pr\left(S_{i,j}^{t+1} = I_h \,\middle|\, S_{i,j}^{t} = I_m\right) = 1 - e^{-\varphi}$.

Markov Chain Model

Agent state transitions are governed by a Markov chain model defined by a set of states and a set of transitions with associated conditional probabilities defining a distribution over the (t+1) possible states. Specifically, the model is a homogenous Markov chain assuming that the transition probabilities are unique, depend only on the current state and not on state history, and are time invariant. A homogenous Markov chain modeling agent state transition can be represented by

(6) $$\boldsymbol{S_{i,j}^{t+1} = P\, S_{i,j}^{t}}$$

where $\boldsymbol{S_{i,j}^{t}}$ is the agent's infection state vector at time *t* of dimension 5 x1. The vector holds a 1 for the state that describes the agent's infection status and zeros for the remaining four states. $\boldsymbol{P}$ is the transition probability matrix read from row (states *H*, E_u, E_d, I_m, I_h at time *t*) to column (states *H*, E_u, E_d, I_m, I_h at time *t*+1).

(7) $$\boldsymbol{P} = \begin{pmatrix} (\mathbf{1}-\boldsymbol{B})^T & \boldsymbol{B}^T & 0 & 0 & 0 \\ 0 & 1-\frac{(x-a)^2}{(b-a)(m-a)} & \frac{(x-a)^2}{(b-a)(m-a)} & 0 & 0 \\ 0 & 0 & (\mathbf{1}-\boldsymbol{C})^T & \boldsymbol{C}^T & 0 \\ 0 & 0 & 0 & e^{-\varphi} & (1-e^{-\varphi}) \\ 0 & 0 & 0 & 0 & 1 \end{pmatrix}$$

The infection state of cell (*i*, *j*) after *n* time steps is given by

(8) $$\boldsymbol{S_{i,j}^{n} = P^{n}\, S_{i,j}^{0}}$$

where $\boldsymbol{S_{i,j}^{0}}$ is the agent's initial 5 x 1 infection state vector. Given that age is deterministic, the composite infection-age state of each cell (*i*, *j*) after *n* time steps is similarly given by

(9) $$\boldsymbol{W_{i,j}^{n} = P^{n}\, W_{i,j}^{0}}$$

where $\boldsymbol{W_{i,j}^{0}}$ is the agent's initial 5 x 1 infection-age state vector.

Time is modeled in discrete monthly time steps. The simulation starts at t=0, representing the vineyard establishment and proceeds until t=600 (year 50). The cell age and infection states are updated after discrete time steps for all cells. So is the infection state of each vine's neighborhood. A monthly time step is probably the most appropriate for a vineyard manager making disease control decisions. Disease diffusion parameters (α and β in table 1) are obtained from a calibration experiment that minimizes the difference in the number of infected vines over time between our simulation results and the results of Charles et al (2009). We choose the lower (0.01/day) and upper bounds (0.2/day) on the parameters in the calibration from transmission rates reported in Tsai et al (2008).[6] We check that the simulated vineyard half-life, defined as the time until 50% disease prevalence, falls within ranges of temporal disease diffusion curves reported in the GLRD literature (Cabaleiro and Segura 2006, Cabaleiro et al. 2008). For other parameters, we choose values from ranges reported in the literature and by consulting experts (table 1).

[Insert table 1 here]

Economic model

Disease diffusion outcomes are mapped into economic outcomes through the damages associated with the disease and the costs incurred when disease control strategies are implemented. The revenue $r_{w_{i,j,t}}$ from a vine located in cell (i,j) that has composite age-infection state $W_{i,j}^{t}$ at time t depends on its infection status and age. A vine is unproductive for τ_{max} time steps (36 months) from planting, after which it reaches its full yield potential. When a grapevine is infected, its yield declines as does the price paid for its grapes due to quality losses.

Disease damage and control

A vineyard manager deciding whether to rogue and replace infected vines considers the costs of disease control relative to disease damages. Disease control costs are: (1) the costs of labor, machinery and material involved in roguing and replacing vines; (2) the opportunity cost of this control measure caused by the forgone revenues between the time control takes place and the time a newly planted vine bears fruit. Disease damages are: (1) the reduction in revenues of uncontrolled infected vines ($r_{w_{i,j,t}}$); (2) the expected losses that those vines will generate by spreading the infection to uninfected vines.

Vine-level disease damage is modeled through a reduction in the per-vine revenue $r_{w_{i,j,t}}$ that depends on the composite age-infection ($w_{i,j,t}$) of a vine located at cell (*i, j*) at time *t*. We choose revenue values (table 2) that build on GLRD literature and interviews with vineyard managers in New York State (Gómez et al 2010; Atallah et al. 2012). For the infection states of *Susceptible*, *Exposed*, *Infective-moderate* and *Infective-high*, yield reductions are 0, 30, 50, and 75 percent, respectively. Quality reduction is reflected in a ten percent reduction in price paid for grapes, regardless of the infection state. Once a grapevine is infected, it transitions through the infection states and remains infected unless rogued and replaced. If rogued and replaced, the age-infection state of a vine is reset to its initial values ($S_{i,j}^{t} = H$ and $A_{i,j}^{t}$=0). Roguing and replacing a grapevine involves a unit cost $c_{u_{i,j}}$ and testing for the virus involves a unit cost $c_{v_{i,j}}$. The vineyard-level revenues and costs at each point in time are the sum of the revenues and costs from each individual grapevine.

[Insert table 2 here]

Vineyard expected net present value

A vineyard manager maximizes the vineyard expected net present value by choosing an optimal disease control strategy from a set of alternatives. Candidate strategies consist of choosing whether to test and/or rogue and replace a vine based on its location and/or infection-age state $W_{i,j,t}$. The optimal strategy is the one that allocates disease control effort over space and time so as to yield the highest vineyard expected net present value among the alternative strategies and the baseline of no control: [7]

(10)

$$\sum_{t\in T, t\geq 0} \rho^t * \{ \sum_{(i,j)\in C} \sum_{w_{i,j}\in S} [r_{w_{i,j,t}} * (1 - \sum_{\tau=0}^{\tau_{max}} u_{w_{i,j,t-\tau}}) - \sum_{\tau=0}^{\tau_{max}} (u_{w_{i,j,t-\tau}} * c_{u_{i,j}}) - (v_{w_{i,j,t}} * c_{v_{i,j}})]\}$$

subject to (9), and:

(11) $r_{w_{i,j,0}} = 0$; $u_{w_{i,j,0}} = 0$; $v_{w_{i,j,0}} = 0$ for all *(i ,j)*

where

ρ^t is the discount factor at time *t* (*t*>0), $\rho^t = 1/(1+r)^t$ and r is the discount rate

$t \in T$ indexes time, where $T=\{0,1,2,\ldots,T_{max}\}$

$\tau \in \{1,2\ldots, \tau_{max}\}$ where τ_{max} is the amount of time it takes a newly planted vine to become productive;

$(i,j) \in C$ indexes cells in row *i* and column *j* of the cellular automaton grid, and *C* is the set of all cells in the grid;

$u_{w_{i,j,t}} \in \{0, 1\}$ is a binary-choice variable equal to one if infected vine in cell (i,j) and state $W_{i,j}$ is rogued (removed) and replaced at time t and zero otherwise ;

$v_{w_{i,j,t}} \in \{0, 1\}$ is a binary-choice variable equal to one if infected vine in cell (i,j) and state $W_{i,j}$ is tested for the virus at time t and zero otherwise ;

$r_{w_{i,j,t}} \in \mathrm{R}_{w_{i,j,t}}$ is the revenue of a vine in cell (i, j) that has age-infection state $W_{i,j}$ at time t; $R_{w_{i,j},t}$ is the space of possible revenues for all states;

$c_{u_{i,j}}$ is the unit cost associated with control variable $u_{w_{i,j},t}$ (removing a vine in cell (i, j) and replacing it with a healthy vine);

$c_{v_{i,j}}$ is the unit cost associated with control variable $v_{w_{i,j},t}$ (testing a vine in cell (i, j) for the virus);

If a vine in state $W_{i,j,t}$ is rogued and replaced at time τ, then $u_{w_{i,j,t-\tau}}$ =1 and the first term in the squared brackets equals zero (i.e. vines that have been planted in the previous τ time units are still unproductive), and the second term takes the value of the roguing and replacement cost. If a vine in state $W_{i,j,t}$ is not rogued and replaced at time τ, then $u_{w_{i,j,t-\tau}}$ =0 for all τ between 0 and τ_{max}, and the first term in the squared brackets takes the value of a vine's revenue, which depends on its age-infection state, and the second term equals zero.

Experimental Design

We design and implement Monte Carlo experiments to evaluate nonspatial and spatial disease control strategies by comparing their bioeconomic outcomes to those under the baseline of no control. Below, we describe the disease control strategies that differ under each Monte Carlo experiment and the bioeconomic outcomes measured.

Disease control strategies

We formulate and evaluate two sets of disease control strategies. The first set is nonspatial and consists of roguing vines based on their symptomatic infection state and their age. The second set takes advantage of the disease diffusion's spatial nature and performs a virus test on

nonsymptomatic vines that are located in the neighborhood of symptomatic ones and then rogues them if they test positive.

We base the set of nonspatial roguing strategies on the six composite age-infection states obtained by interacting the latency-defined age categories (*Young*: 0-5; *Mature*: 6-19; *Old*: 20 and above) with the symptomatic infection categories (I_m and I_h).The strategies are compared to a baseline case of no control. The infection-age control strategies are then: no disease control (baseline case); roguing and replacing vines that are *Infective-moderate* and *Young* (strategy I_mY); *Infective-moderate* and *Mature* (strategy I_mM); *Infective-moderate* and *Old* (strategy I_mO); *Infective-high* and *Mature* (strategy I_hM); and, *Infective-high* and *Old* (strategy I_hO). [8] Finally, we include three additional disease control scenarios that target grapevines in one of the three infection states regardless of age. We do so to examine the impact of age-structured control strategies on disease diffusion and control cost-effectiveness, compared to their nonage-structured counterparts.

Among the set of spatial strategies, one consists in roguing and replacing symptomatic vines $V_{i,j}$ in addition to testing their two within-column neighbors (vines $V_{i-1,j}$ and $V_{i+1,j}$ in figure 1.a) and roguing them if they test positive (strategy I_mNS). The other strategy also rogues and replaces symptomatic vines $V_{i,j}$ but it tests four within-column neighbors ($V_{i-2,j}$, $V_{i-1,j}$, $V_{i+1,j}$, $V_{i+2,j}$ in figure 1.b.) and two across-column neighbors ($V_{i,j-1}$ and $V_{i,j+1}$ in figure 1.b.) and rogues them if they test positive (strategy I_mNS2EW). There is a unit testing cost, $c_{v_{i,j}}$, associated with the labor and material used in testing vines for a grapevine leafroll-associated virus (table 2). Given that *Exposed* vines become detectible by a virus test (i.e. they transition from E_u to E_d) only after a certain undetectability period (with minimum *a*, maximum *b* and mode *m*, table 2), vines in state

E_u will falsely test negative, creating a situation of imperfect information in disease control that precludes disease eradication.

Monte Carlo experiments

Each experiment consists of a set of 1,000 simulation runs, over 600 months, on a vineyard of 5,720 grapevines. Experiments differ in the disease control strategies they employ. Outcome realizations for a run within an experiment differ due to random spatial initialization, and random spatial disease diffusion. Data collected over simulation runs are the probability density functions of the bioeconomic outcomes under each strategy.

Bioeconomic outcomes measured and ranking of control strategies

In order to analyze the impact of strategies on disease diffusion, we use the vineyard expected half-life. The latter is defined as the expected period it takes for the total number of healthy vines to decrease by half, or the time it takes for the disease to reach 50% prevalence. From the biological part of the model, the desired disease control strategies are those that increase the half-life the most, compared to the baseline case of no control. In order to find the optimal disease control among those considered, we employ the objective function (Equation 10) to rank the vineyard net present value distributions under the alternative strategies using a first-order stochastic dominance test.[9] The objective function takes into account the total amount of control realized under each strategy to achieve the half-life increase but also the timing, intensity and location of that control. In addition, we collect data on the expected average vineyard age and the distribution of the cumulative number of grapevines rogued and replaced, for each of the two spatial strategies considered.

Results and Discussion

We find that, when virus testing is not employed to uncover the state of nonsymptomatic vines, the nonspatial strategy of roguing young moderately infected vines yields the highest vineyard expected net present value. However, if virus testing is used, the spatial strategy that involves testing-and-roguing two within-column neighbors of a symptomatic vine maximizes the vineyard expected net present value compared to all other disease control strategies and the baseline.

Nonspatial strategies

Our age-structured simulations indicate that the vineyard's expected net present values over a 50-year period are greatest when young, moderately infected vines are targeted. The I_mY roguing strategy achieves an economic improvement of 5% over the baseline (table 3). This improvement is statistically significant at the 1% level. The I_mM strategy's ENPV is, however, only marginally higher than the baseline. Targeting moderately infected vines at a young age delays vineyard half-life by 41 months over the baseline. Waiting until a vine is mature before removing it reduces that benefit to 25 months which in turn decreases the economic benefit to less than 1% over the baseline. The temporal disease diffusion curves in figure 2 illustrate why targeting young vines (I_mY) achieves higher vineyard half-life than targeting mature vines[10]. Disease control, visible as dips in the red curve and peaks in the green curve in figures 2b and 2c, occurs more frequently under the I_mY strategy than under the I_mM strategy. With the latter strategy, disease control is delayed until newly infected vines mature (5 to 20 years). Figure 3 illustrates how more frequent roguing and replacement under the I_mY strategy (panel b) compares to the I_mM strategy (panel c): the I_mY strategy achieves lower disease prevalence (more *Healthy* vines in dark green).

[Insert table 3 here]

[Insert figure 2 here]

[Insert figure 3 here]

Although a vineyard manager might be inclined to wait until a productive vine is more infected and/or older before roguing and replacing it in order to reap greater grape production, doing so reduces the ENPV of the vineyard and is only a marginal improvement over no control at all. Strategies targeting old and/or highly infected vines (strategies I_mO, I_hM, I_hO) all yield ENPVs that are lower than the baseline (table 3). In fact, any strategy consisting of roguing old vines is unsuccessful at extending the vineyard's expected half-life relative to the baseline, regardless of the infection states targeted. Moreover, strategies targeting heavily infected vines do not delay disease spread by more than 5 or 9 months. Such strategies have the drawback of waiting longer to control disease diffusion because of the time period (parameter *Inf* in table 2) it takes a vine to transition from state I_m to state I_h and/or the time it takes vines to reach the *Old* state. The results suggest that, no matter the cost of disease control, roguing and replacing old and/or heavily infected vines alone is not recommended given that they yield little or no increase in vineyard half-life.

Simulations of the strategy that targets all age categories yield an expected net present value that is 11.7% lower than the baseline, in spite of being the best in extending the half-life of the vineyard (42% increase in expected half-life, table 3). This finding highlights the importance of age-structuring disease control strategies. By focusing on young, moderately infected vines, a more effective disease control policy involving less roguing leads to a better economic outcome when compared to a strategy that does not discriminate based on age.

Spatial strategies

The vineyard expected net present values under the spatial strategies are greater than those obtained under their nonspatial counterparts. Economic improvements over the baseline are of

the order of 24% and 39% (table 3) for the I_mNS2EW and I_mNS strategies, respectively. These improvements underscore the superiority of spatial over nonspatial, age-structured disease control. These spatial strategies increase ENPV by uncovering the infection state of nonsymptomatic grapevines situated in the neighborhood of a symptomatic grapevine. They delay the vineyard half-life to years beyond the maximum model time T_{max} (figures 2d and 2f). The vineyard half-life is not reached until after around 1,600 simulation months (approximately 133 years) for the I_mNS2EW strategy (figure 2g) and 2,000 simulations months (approximately 167 years) for the I_mNS strategy (figure 2e). The *Infected-high* state is never reached (see the temporal disease diffusion curves in figures 2d-2f and the spatial disease diffusion snapshots in figures 3d and 3e). Both strategies control the disease within similar upper and lower bounds and the oscillations do not dampen in the long run under either strategy (figures 2e and 2g). Surprisingly, the strategy that tests only the two within-column neighbors of a moderately infected vine, strategy I_mNS (figure 2d), is better at controlling the disease than the strategy that tests the four within-column neighbors and two across-column neighbors, strategy I_mNS2EW (figure 2f). This is counterintuitive since one would expect that the identification of more infected, nonsymptomatic vines (*Exposed*) and their removal before they become *Infective* would slow disease diffusion further. However, grapevine roguing and replacement implies replacing infected grapevines with younger healthy ones that have short latency periods. That is, once newly planted young vines get infected, they become infectious in a relatively short period, and contribute to further disease diffusion.

To test if this explanation is consistent with the experimental data, we compare the expected vineyard age and the expected total number of grapevines removed and replaced under the two strategies. We find that the I_mNS2EW strategy, by scouting farther along columns for

Exposed nonsymptomatic vines and including across-column neighbors in the search, causes the final amount of roguing to be almost twice as large as it is under the I_mNS strategy (figure 4). In their analytical model of roguing and replanting, Chan and Jeger (1994) also found that higher replanting rates made the disease more difficult to eradicate, suggesting a tradeoff between roguing and replanting in designing optimal disease management strategies. We find that this larger level of roguing and replanting causes the vineyard's average age to be lower under the I_mNS2EW strategy than under the I_mNS strategy. The expected difference in age is 3.1 (±0.03) years by the 300th simulation month (i.e., by the 25th year). This expected age difference increases over time and reaches 7.3 (± 0.16) years by the 600th month (i.e., by year 50).

[Insert figure 4 here]

The cumulative density function (CDF) plots in figure 5 show that, among the disease control strategies considered, roguing and replacing symptomatic vines while testing and roguing their within-column neighbors (I_mYNS) is optimal. This strategy first-order stochastically dominates all the others. Both spatial test-and-rogue strategies ($I_mYNS2EW$, I_mYNS) first-order stochastically dominate age-structured strategies (I_mY and I_mM). Among the age-structured strategies, the one targeting moderately infected and young vines (I_mY) dominates the strategy of roguing moderately infected and mature vines (I_mM). The latter strategy does not dominate the baseline as can be seen by the intersection of their CDFs.

[Insert figure 5 here]

Disease control strategies yield different results through their different allocation of disease control effort over time and space. A manager deciding when and where to control GLRD (i.e., what age, infection, and location states to target) faces tradeoffs between the ecological benefits and drawbacks of controlling earlier and more frequently. The superiority of

I_mNS over *I_mNS2EW* indicates that testing and roguing the two more distant within-column neighbors and two across-column direct neighbors will reduce the ENPV and actually speed the GLRD diffusion through a younger vineyard. The economic determinants of disease control allocation over space and time are the direct control costs, the opportunity cost of disease control, the reduced production and quality of grapes, and the manager's discount rate. Disease control decisions involve economic tradeoffs among these determinants. Two types of costs incentivize a vineyard manager to postpone roguing depending on her discount rate. Those are the direct control costs, labor, machinery and material costs involved in testing, roguing and replacing vines ($c_{u_{i,j}}$ and $c_{v_{i,j}}$), and the opportunity cost of roguing an infected but still-productive vine. The latter cost consists of the forgone revenues during the time newly planted vines are still unproductive. Postponing those costs has to be balanced with two types of ensuing damages: one is the continued reduction in revenues of uncontrolled infected vines ($r_{w_{i,j,t}}$) and the other is the expected economic losses that those vines generate by spreading the infection to uninfected vines. The results under the parameters considered in this article show that, for the strategies evaluated, it is worthwhile to incur the costs of disease control earlier in order to avoid future damages and to reap the benefits of a longer vineyard life later. That is, for nonspatial strategies, it is better to target younger vines in their earlier infection stages than older vines. For spatial strategies, testing the neighborhood of symptomatic vines reduces the amount of uncertainty by revealing the state of neighboring nonsymptomatic vines. Incurring the virus testing costs is justified by a higher ENPV over the lifetime of the vineyard. Sensitivity analyses of the model to the unit virus test cost show that even if the cost were $30 (instead of $2.6), the winning spatial strategy (*I_mNS*) remains optimal, achieving an economic improvement of 29% over the baseline (table 4), much ahead of the winning nonspatial strategy *I_mY* (5%) (table 3). At

a testing cost of $30 per vine, the $I_mYNS2EW$ strategy is no longer cost-effective. Its ENPV is 3% lower than the baseline. Optimality of the winning strategy is not sensitive to a threefold-increase in the cost of roguing and replanting. Both spatial control strategies retain their stochastic dominance over the nonspatial strategies.

[Insert table 4 here]

Conclusions and Directions for Future Research

There is growing interest in research dealing with the economics of integrated spatial-dynamic processes. This article features a computational bioeconomic model of disease diffusion and control. This approach addresses some of the limiting assumptions in previous work by allowing for agent heterogeneity and fully characterizing disease spatial-dynamic processes. We apply this model to grapevine leafroll disease and evaluate alternative disease control strategies using stochastic dominance tests. The simulation results are valuable for vineyard managers, suggesting that roguing and replanting is not cost-effective if mature or old vines are targeted. Most importantly, the simulation results show that the spatial strategy of roguing symptomatic vines and testing-and-roguing their two within-column neighbors, dominates all other disease control strategies. It does so by uncovering the infection state of a proportion of nonsymptomatic grapevines situated in the neighborhood of symptomatic vines.

The results show a general feature of spatial-dynamic processes: optimal policy interventions are those that achieve the temporally, spatially, and quantitatively optimal allocation of inputs. In this model, optimal timing for roguing and replacing individual grapevines is determined by their young age and moderate levels of infection. Optimal spatial allocation of disease control involves testing-and-roguing the two within-column neighbors of

young, moderately infected vines. However, we found that expanding the spatial allocation of disease control to four within-column neighbors and two across-column neighbors cause the amount of disease control to reach a threshold that causes the vineyard average age to decrease. This, in turn, increases the rate of disease diffusion due to the lower latency period of young replants. The model results highlight the temporal, spatial, and quantitative tradeoffs between and within the ecological and economic components of spatial-dynamic complex adaptive systems in general and disease systems in particular.

This model can be adapted to disease management in other high-value horticultural crops that are characterized by within-farm variation in physical, chemical or biological factors affecting individual plant growth and health. This variability justifies agent-based management. Such crops include citrus trees, where precision agriculture has been employed to detect diseases (Pydipati, Burks, and Lee 2006), and other fruit tree crops, where reflectance imaging has been employed to detect insect infestations (Wang et al. 2011).

This work does not model negative spatial externalities such as the ones that would occur due to the flow of vectors from neighboring infected vineyards left uncontrolled. Further research should model such situations, formulate and evaluate spatial strategies that are able to control the disease diffusion not only within the vineyard but also across vineyards. We expect this situation to yield strategies that alter the spatial configuration of the vineyard in a way that slows down disease diffusion. Establishing “fire breaks” from an adjacent, infected vineyard may result in losses in yields that will need to be measured against the value of lower disease damages in the future. If cost-efficient, these designs might be recommended for the establishment of more disease-resistant vineyards and orchards with higher ENPV.

References

Akanle, O. M., and Zhang, D. Z. (2008). Agent-based model for optimising supply-chain configurations. *International Journal of Production Economics*, *115*(2), 444-460

Arthur, W. B. 2006. "Out-of-equilibrium economics and agent-based modeling". In *Agent-Based Computational Economics. Handbook of Computational Economics*, vol. 2. Tesfatsion, L., Judd, K. (Eds.). Elsevier, North-Holland

Atallah, S.S., M. I. Gómez, M. F. Fuchs, and T. E. Martinson. 2012. "Economic Impact of Grapevine Leafroll Disease on Vitis vinifera cv. Cabernet franc in Finger Lakes Vineyards of New York." *American Journal of Enology and Viticulture* 63:73-79

Babcock, B. A., E. Lichtenberg, D. Zilberman. 1992. "Impact of Damage Control and Quality of Output: Estimating Pest Control Effectiveness." *American Journal of Agricultural Economics* (74), no. 1, 163-172

Beach, R. H., Poulos, C., and S. K. Pattanayak. 2007. "Agricultural household response to avian influenza prevention and control policies." *Journal of Agricultural and Applied Economics*, *39*(2), 301.

BenDor, T., J. Scheffran, and B. Hannon. 2009. "Ecological and economic sustainability in fishery management: A multi-agent model for understanding competition and cooperation." *Ecological Economics* (68), 1061–1073

Berger, T. 2001. "Agent-based spatial models applied to agriculture: a simulation tool for technology diffusion, resource use changes and policy analysis." *Agricultural Economics* 25, no. 2-3: 245-260

Brauer, F., and C. Castillo-Chavez. 2001. Mathematical Models in Population Biology and Epidemiology, *Texts in Applied Mathematics* 40, Springer-Verlag, New York

Cabaleiro, C., C. Couceiro, S. Pereira, M. Barrasa, and A. Segura. 2008. “Spatial analysis of epidemics of Grapevine leafroll associated virus-3.” *European Journal of Plant Pathology* 121:121-130

Cabaleiro, C. and A. Segura. 2007. “Some characteristics of the transmission of grapevine leafroll associated virus 3 by Planococcus citri Risso.” *European Journal of Plant Pathology* 103, no. 4: 373-378.

——. 2006. “Temporal analysis of grapevine leafroll associated virus 3 epidemics.” *European Journal of Plant Pathology* 114:441–446

Chan, M-S, and M. J. Jeger. 1994. “An Analytical Model of Plant Virus Disease Dynamics with Roguing and Replanting.” *Journal of Applied Ecology* 31, no. 3: 413-27

Charles, J., K. Froud, R. van den Brink, and D. Allan. 2009. “Mealybugs and the spread of Grapevine leafroll-associated virus 3(GLRaV-3) in a New Zealand Vineyard.” *Australasian Plant Pathology* 6:576-83

Charles, J., D. Cohen, J. Walker, S. Forgie, V. Bell and K.Breen. 2006. “A review of the ecology of grapevine leafroll associated virus type 3 (GLRaV-3).” *New Zealand Plant Protection* 59:330-337

Constable, F.E., Connellan, J., Nicholas, P. and B. C. Rodoni. 2012. “Comparison of enzyme linked immunosorbent assays and reverse-transcription polymerase chain reaction for the reliable detection of Australian grapevine viruses in two climates during three growing seasons.” *Australian Journal of Grape and Wine Research* 18, 239–244.

Diagnostics, A.C. 2012. *ELISA tests for Plant Viruses: Grapevine leafroll-associated virus - 3 (GLRaV-3) - DAS ELISA*. Available at http://www.acdiainc.com/GLRaV-3.htm. Last accessed 10/12/2012.

Epanchin-Niell, R. S. and J.E. Wilen. 2012. “Optimal spatial control of biological invasions.” *Journal of Environmental Economics and Management* 63: 260-270

Fagiolo, G., Birchenhall, C., & Windrum, P. 200). “Empirical validation in agent-based models: Introduction to the special issue.” *Computational Economics*, *30*(3), 189-194.

Fenichel, E. P. and Horan R. D. 2007. “Gender-Based Harvesting in Wildlife Disease Management.” *American Journal of Agricultural Economics* 89 (4):904-920

Fuchs, M., P. Marsella-Herrick, G.M. Loeb, T.E. Martinson, and H.C. Hoch. 2009. “Diversity of ampeloviruses in mealybug and soft scale vectors and in grapevine hosts from leafroll-affected vineyards.” *Phytopathology* 99:1177-1184.

Gilbert, N. and P. Terna. 2000. “How to build and use agent-based models in social science.” *Mind and Society* 1, no. 1: 57-72

Golino, D.A., E. Weber, S.T. Sim, and A. Rowhani. 2008. “Leafroll disease is spreading rapidly in a Napa Valley vineyard.” *California Agriculture* 62:156-160.

Goheen, A.C., and J.A. Cook. 1959. “Leafroll (red-leaf or rougeau) and its effects on vine growth, fruit quality, and yields”. *American Journal of Enology and Viticulture* 10:4:173-181

Gómez, M., Atallah S., Fuchs M., Martinson T., and White G., 2010. “Economic impact of the grape leafroll virus (GLRV) in the Finger Lakes region of New York.” *Extension Bulletin No. EB-2010-15*, Charles H. Dyson School of Applied Economics and Management , Cornell University

Greenhalgh, D. 2011. “Age-structured models and optimal control in mathematical epidemiology: a survey.” In *Optimal Control of Age-Structured Populations in Economy,*

Demography, and the Environment. Routledge Explorations in Environmental Economics. Boucekkine,R, N. Hritonenko and Y. Yatsenko (eds.), Routledge.

Greenhalgh, D. 1986. "Control of an Epidemic Spreading in a Heterogeneously Mixing Population". *Mathematical Biosciences* 80:23-45

Habili, N., C. F. Fazeli, A. Ewart, R. Hamilton, R. Cirami, P. Saldarelli, A. Minafra, and M. A. Rezaian. 1995. "Natural spread and molecular analysis of grapevine leafroll-associated virus 3 in Australia." *Phytopathology* 85, no. 11: 1418

Hall, D. C. and R. B. Norgaard. 1973. "On the timing and application of pesticides." *American Journal of Agricultural Economics* 55, 198-201

Horan, R. D., E. P. Fenichel, C. A. Wolf, and B. M. Gramig. 2010. "Managing infectious animal disease systems." *Annual Review of Resource Economics* 2:101-124

Horan, R.D., and C.A. Wolf. 2005. "The Economics of Managing Infectious Wildlife Disease." *American Journal of Agricultural Economics* 87(3): 537–551

Jooste, A. E. C., G. Pietersen and J. T. Burger. 2011. "Distribution of grapevine leafroll associated virus-3 variants in South African vineyards." *European Journal of Plant Pathology* 131:371–381

Sun, J. and L. Tesfatsion. 2007. Dynamic Testing of Wholesale Power Market Designs: An Open-Source Agent-Based Framework. *Computational Economics* vol. 30 no. 3: 291-327

Kotz, S. and J. Rene van Dorp. 2004. *Beyond Beta Other Continuous Families of Distributions with Bounded Support and Applications,* Singapore: World Scientific 289 pp.

Luminex 2010. "Overcoming the Cost and Performance Limitations of ELISA with xMAP® Technology. xMAP® Technology." *Technical Note*. Luminex Corporation, Austin, Texas.

Macal, C. M. and M. J. North. 2010. “Tutorial on agent-based modeling and simulation.” *Journal of Simulation* 4: 151-162

Martelli, G.P., and E. Boudon-Padieu. 2006. “Directory of infectious diseases of grapevines. International Centre for Advanced Mediterranean Agronomic Studies.” *Options Méditerranéennes* Ser. B, Studies and Research 55:59-75.

Martin, R.R., K.C. East well, A. Wagner, S. Lamprecht, and I.E. Tzanetakis. 2005. “Survey for viruses of grapevine in Oregon and Washington. *Plant Disease*.” 89:763-766.

Martinson, T.E., M. Fuchs, G. Loeb, and H.C. Hoch. 2008. “Grapevine leafroll: An increasing problem in the Finger Lakes, the US and the world.” *Finger Lakes Vineyard Notes* 6:6-11.

Medlock, J., and A. P. Galvani. 2009. “Optimizing influenza vaccine distribution.” *Science* 325, no. 5948: 1705-1708.

Miller, J. H. and S. E. Page, .2007. “Complex Adaptive Systems: An Introduction to Computational Models of Social Life.” Princeton University Press

Naidu, R., A., E. M. Perry, F. J. Pierce, and T. Mekuria. 2009. “The potential of spectral reflectance technique for the detection of Grapevine leafroll-associated virus-3 in two red-berried wine grape cultivars.” *Computers and Electronics in Agriculture* 66, no. 1: 38-45.

Osgood, N. 2007. “Using Traditional and Agent Based Toolsets for System Dynamics: Present Tradeoffs and Future Evolution.” *System Dynamics*, 2007.

Pietersen, G. 2006. “Spatio-temporal dynamics of grapevine leafroll disease in Western Cape vineyards.” *Extended Abstracts,* 15th Meeting of the International Council for the Study of Virus and Virus-like Diseases of the Grapevine, 2006. Stellenbosch, South Africa, pp 126-127.

Pietersen G., 2004. “Spread of Grapevine leafroll disease in South Africa- a difficult, but not insurmountable problem.” *Wynboer Technical Yearbook 2004/5*

Pydipati, R., T. F. Burks, and W. S. Lee. 2006. “Identification of citrus disease using color texture features and discriminant analysis.” *Computers and Electronics in Agriculture* 52(1), 49-59.

Railsback, S. F., and V. Grimm. 2011. *Agent-based and individual-based modeling: A practical introduction*. Princeton University Press.

Rahimiyan, M., and Rajabi Mashhadi, H. 2010. Evaluating the efficiency of divestiture policy in promoting competitiveness using an analytical method and agent-based computational economics. *Energy Policy*, *38*(3), 1588-1595.

Rahmandad, H. and J. Sterman. 2008. “Heterogeneity and Network Structure in the Dynamics of Diffusion: Comparing Agent-Based and Differential Equation Models.” *Management Science*, 54(5):998–1014

Sanchirico, J. and J. Wilen. 1999. “Bioeconomics of spatial exploitation in a patchy environment.” *Journal of Environmental Economics and Management* 37: 129-150

——. 2005. “Optimal spatial management of renewable resources: matching policy scope to ecosystem scale.” *Journal of Environmental Economics and Management* 50: 23–46

Saphores, J.D.M. 2000. “The economic threshold with a stochastic pest population: a real options approach.” *American Journal of Agricultural Economics* 82: 541–555.

Schneckenreither, G., N. Popper, G. Zauner, and F. Breitenecker. 2008. “Modelling SIR-type epidemics by ODEs, PDEs, difference equations and cellular automata–A comparative study.” *Simulation Modelling Practice and Theory* 16, no. 8: 1014-1023.

Smith, M. D., J. N. Sanchirico, and J. E. Wilen. 2009. “The economics of spatial-dynamic processes: applications to renewable resources.” *Journal of Environmental Economics and Management* 57, no. 1: 104-121.

Tahvonen, O. 2010. Age-structured optimization models in fisheries bioeconomics: a survey. In *Optimal Control of Age-Structured Populations in Economy, Demography, and the Environment*. Routledge Explorations in Environmental Economics. Boucekkine,R, N. Hritonenko and Y. Yatsenko (eds.), Routledge.

Teose, M., K. Ahmadizadeh, E. O'Mahony, R. L. Smith, Z. Lu, S. E. Ellner, C. Gomes, Y. Grohn 2011. “Embedding System Dynamics in Agent Based Models for Complex Adaptive Systems”. Twenty-Second International Joint Conferences on Artificial Intelligence, Barcelona, Spain, July 16-22, 2011

Tesfatsion, L., and K. L. Judd (ed.). 2006. *Handbook of Computational Economics*, Elsevier, edition 1, volume 2, number 2

Tsai, C.W., A. Rowhani, D.A. Golino, K.M. Daane, and R.P.P. Al-meida. 2010. “Mealybug transmission of grapevine leafroll viruses: An analysis of virus-vector specificity.” *Phytopathology* 100:830-834.

Tsai, C-W., J. Chau, L. Fernandez, D. Bosco, K. M. Daane, and R. P. P. Almeida. 2008. "Transmission of Grapevine leafroll-associated virus 3 by the vine mealybug (Planococcus ficus)." *Phytopathology* 98, no. 10: 1093-1098.

Wang, J., Nakano, K., Ohashi, S., Kubota, Y., Takizawa, K., & Sasaki, Y. 2011. “Detection of external insect infestations in jujube fruit using hyperspectral reflectance imaging.” *Biosystems Engineering*, *108*(4), 345-351.

Wilen, J. 2007. “Economics of spatial–dynamic processes.” *American Journal of Agricultural Economics* 89: 1134–1144.

Wolf, T. K. 2008. *Wine Grape Production Guide for Eastern North America*. Natural Resource, Agriculture, and Engineering Service (NRAES) Cooperative Extension, Ithaca, NY

White, G. 2008.*Cost of establishment and production of vinifera grapes in the Finger Lakes region of New York*. College of Agriculture and Life Sciences, Cornell University, Ithaca, NY

White, R., and G. Engelen. 2000. “High-resolution integrated modeling of the spatial dynamics of urban and regional systems.” *Computers, Environment and Urban Systems* 24: 383-400.

Table 1. **Aggregate and Agent-Based Models**

Aggregate models	*Agent-Based models*
Top-down	Bottom-up
Precise	Precise and flexible
Focus on equilibrium states	Equilibrium and out-of-equilibrium states
1, 2, or infinite number of agents	1, 2, …, *N* agents
Nonspatial or partially-spatial	Fully spatial
Homogenous agents	Heterogeneous agents

Adapted from Arthur (2006) and Miller and Page (2007)

Table 2. Model Parameters

Parameter	Description	Value	Unit	Sources
α	within-column rate of transition from H to E_u	4.2*	month $^{-1}$	Model calibration to data in Charles et al (2009) with validation using data in Cabaleiro and Segura (2006) and Cabaleiro et al (2008);
β	across-column rate of transition from H to E_u	0.014*	month $^{-1}$	
L_y	latency period for young vines	24	months	Age-specific latency periods constructed based on latency period in Jooste, Pietersen, and Burger (2011)
L_m	latency period for mature vines	48	months	
L_o	latency period for old vines	72	months	
a	Minimum of virus undetectability period	4	months	Cabaleiro and Segura 2007; Constable et al. (2012)
b	Maximum of virus undetectability period	18	months	
m	Mode of virus undetectability period	12	months	
Inf	period spent in state I_m before a vine transitions to state I_h	36	months	M. Fuchs, personal communication, April 9, 2012
τ_{max}	period from planting until productivity	36	months	White (2008)
T_{max} ,A_{max}	maximum model time, maximum vine age	600	months	White (2008)
ρ	discount factor	0.9959	month $^{-1}$	Assumed. Equivalent to an annual discount rate of 5%
$c_{u_{i,j}}$	unit cost of vine roguing (removal) and replacement	7.25	\$/vine	Based on White (2010) and Atallah (2012)
$c_{v_{i,j}}$	unit cost of vine virus testing	2.61	\$/vine	AC Diagnostics (2012) for the material cost based on 1,000 samples; Luminex (2010) for the labor time
$r_{w_{i,j,},t}$	revenue of a vine in age-infection state			Vine revenue is based on vine value for Cabernet franc (White 2008) and vine value reduction (Atallah 2012 and references therein).
	$A_{i,j}^t \leq 3$	0	\$/vine	
	$A_{i,j}^t \geq 4$ and $S_{i,j}^t = H$	5.12	\$/vine	
	$A_{i,j}^t \geq 4$ and $S_{i,j}^t = E$	3.22	\$/vine	
	$A_{i,j}^t \geq 4$ and $S_{i,j}^t = I_m$	2.30	\$/vine	
	$A_{i,j}^t \geq 4$ and $S_{i,j}^t = I_h$	1.15	\$/vine	

* Transition rates are constant for a particular location over the 50 year period of study. This excludes for instance situations where new insect vector species are introduced and contribute to an increase in transmission rates.

Table 3 Disease Control Strategies: Expected Vineyard Half-life and Expected Net Present Value

Disease Control Strategies			Expected half-life [a]			Expected net present value [a]		
			Value	Improvement over baseline [b]		Value	Improvement over baseline	
			months	*months*	*%*	*million $*	*1,000 $*	*%*
Baseline, no control			188 (8)[c]	-		3.336 (0.053)	-	-
Nonspatial strategies								
Age-structured								
Symptoms severity	*Age*	*Acronym*						
Moderate	Young	I_mY	229 (7)	41***	22	3.517 (0.046)	181***	5
Moderate	Mature	I_mM	213 (8)	25 ***	13	3.345 (0.053)	9***	0
Moderate	Old	I_mO	188 (8)	0	0	3.283 (0.054)	-53***	-2
High	Mature	I_hM	193 (10)	5 ***	3	3.243 (0.052)	-92***	-3
High	Old	I_hO	188 (08)	0	0	3.321 (0.054)	-15***	0
Not-age-structured								
Moderate	All	I_m	267 (8)	79***	42	2.945 (0.064)	-391***	-12
High	All	I_h	197 (11)	9***	5	3.194 (0.058)	-141***	-4
Spatial (neighborhood-based) strategies								
Two within-column neighbors		*NS*	2,533 (222)	2,345***	1,249	4.650 (0.050)	1,314 ***	39
Four within-column and two across-column neighbors		*NS2EW*	1,639 (146)	1,452***	773	4.153 (0.044)	817 ***	24

[a] Expectations are obtained from 1,000 simulations; [b] Improvement = mean (scenario)-mean (baseline); [c] Standard deviations in parentheses; *** Difference is significant at the 1% level using estimations with robust standard errors.

Table 4. **Sensitivity of the Expected Net Present Value to the Unit Virus-Test Cost**

Spatial strategies	Acronym	Virus-test unit cost $c_{v_{i,j}}$	Expected net present value [a] Value	Improvement over baseline [b]	
		$/vine	*million $*	*million $*	*%*
Within-column neighbors	*NS*	2.6	4.650 (0.050)[c]	1.314 ***	39
		30	4.294 (0.075)	0.958 ***	29
Within and across-column neighbors	*NS2EW*	2.6	4.153 (0.044)	0.817 ***	24
		30	3.221 (0.074)	-0.115 ***	-3

[a] Expectations are obtained from 1,000 simulation; [b] Improvement = mean (scenario)- mean (baseline); [c] Standard deviations in parentheses; *** Difference is significant at the 1% level using estimations with robust standard errors.

Figure 1: Types of grapevine neighborhood

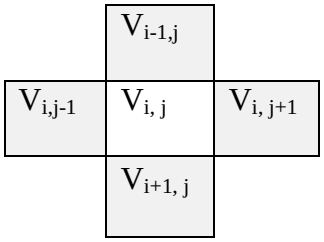

Figure 1a: von Neumann neighborhood of vine $V_{i,j}$

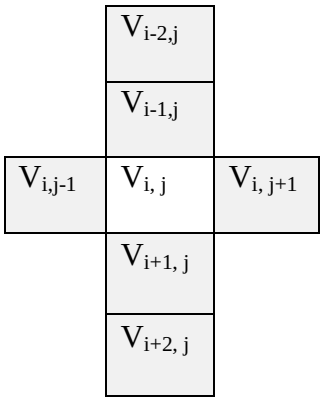

Figure 1b: Vines in the neighborhood of vine $V_{i,j}$ that are targeted under the $I_m NS2EW$ strategy

Figure 2: Single realizations of temporal disease diffusion

Figure 2a: Baseline case

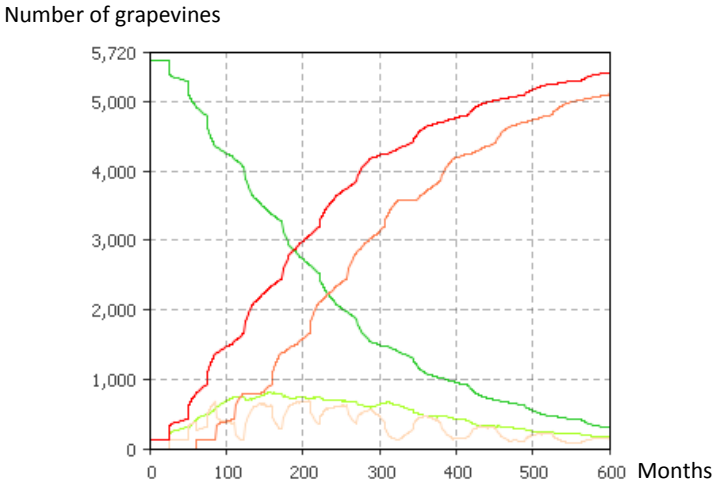

Figure 2b: I_mY control strategy

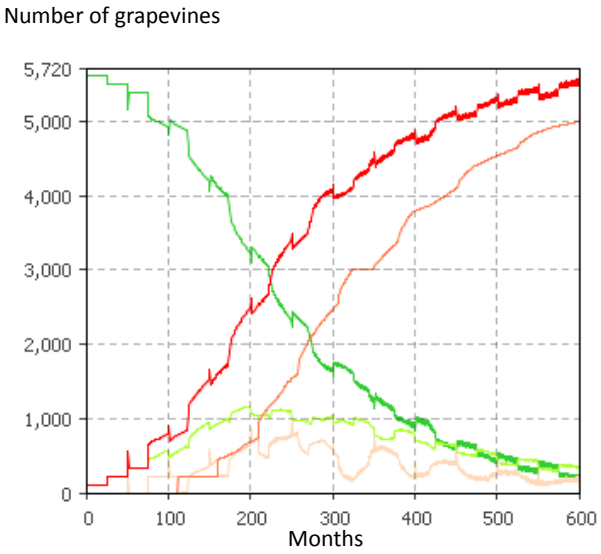

Figure 2c: I_mM control strategy

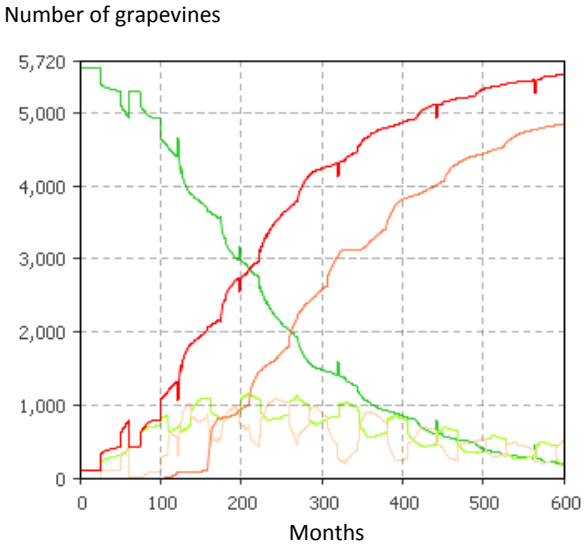

Figure 2d: I_mNS control strategy

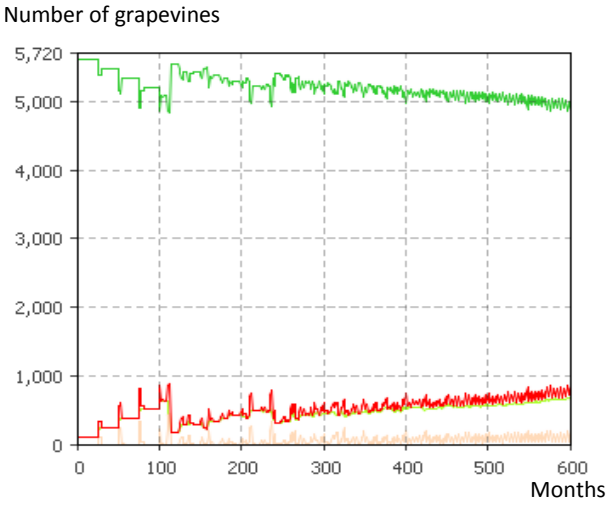

Figure 2e: I_mNS control strategy in the long run

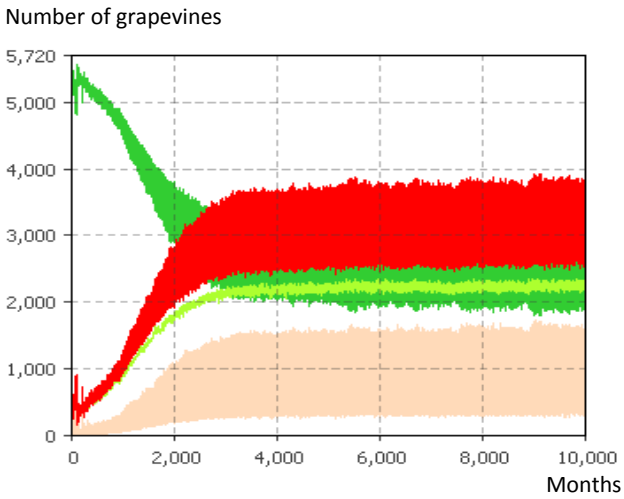

Figure 2f: I_mNS2EW control strategy

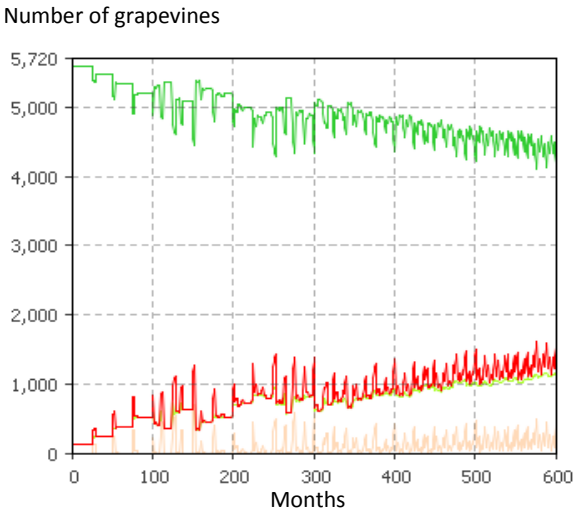

Figure 2g. I_mNS2EW strategy in the long run

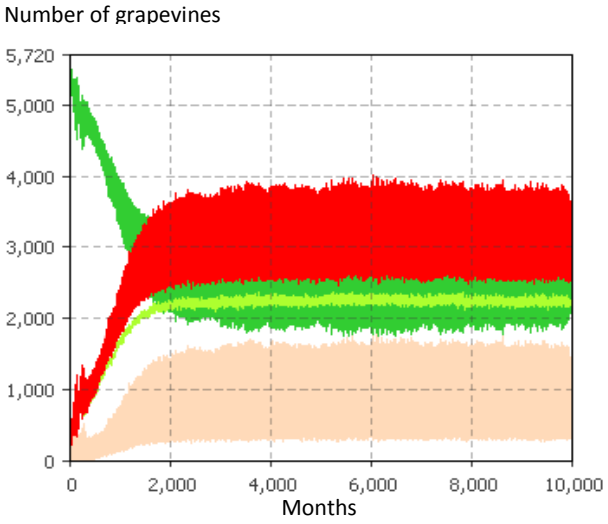

Legend:

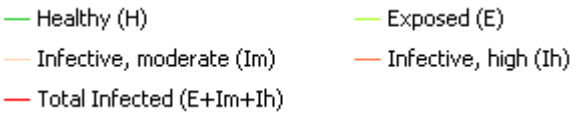

Figure 3: Single realizations of the spatial disease diffusion in a vineyard at t=200 months

Figure 3a: Baseline case

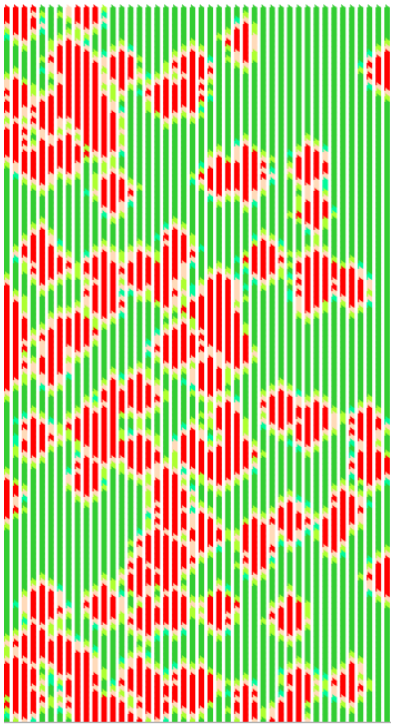

Figure 3b: I_mY strategy

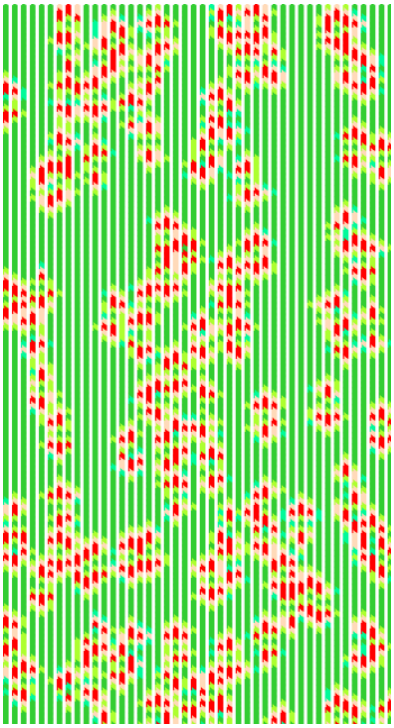

Figure 3c: I_mM strategy

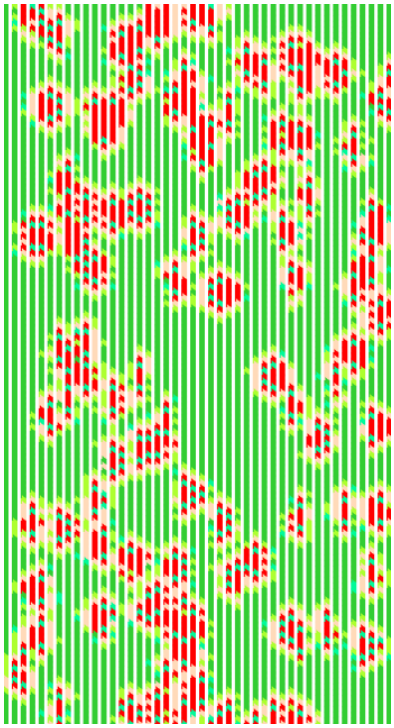

Figure 3d: I_mNS strategy

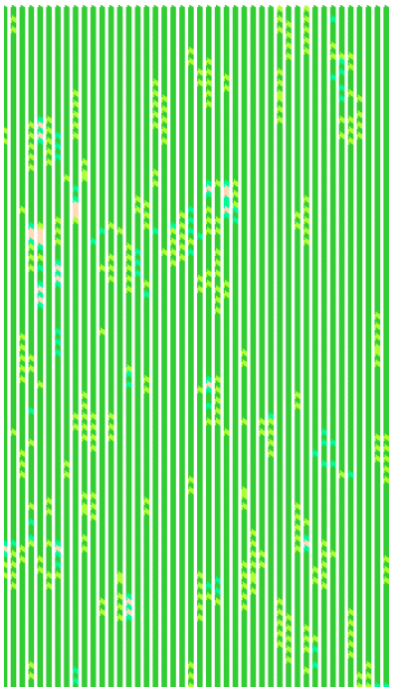

Legend

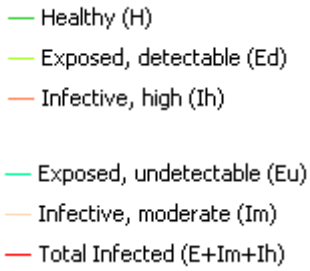

Figure 3e: I_mNS2EW strategy

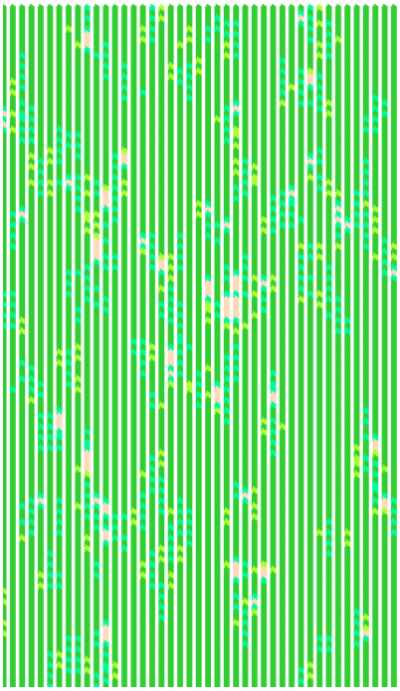

Figure 4: Two-dimensional histogram of the cumulative number of grapevines removed and replaced (y-axis) over time (x-axis). Darker color indicates higher frequency.

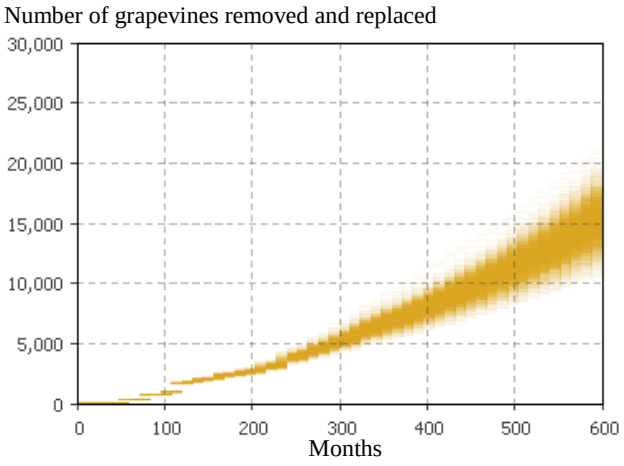

Figure 4a: I_mNS control strategy

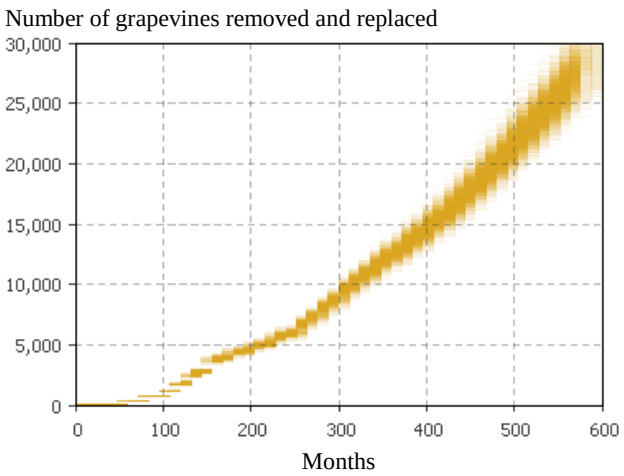

Figure 4b: I_mNS2EW control strategy

Figure 5: First-order stochastic dominance test of net present values (million $) over 50 years: baseline, age-structured (I_mM, I_mY) and spatial (I_mNS, I_mNS2EW) disease control strategies

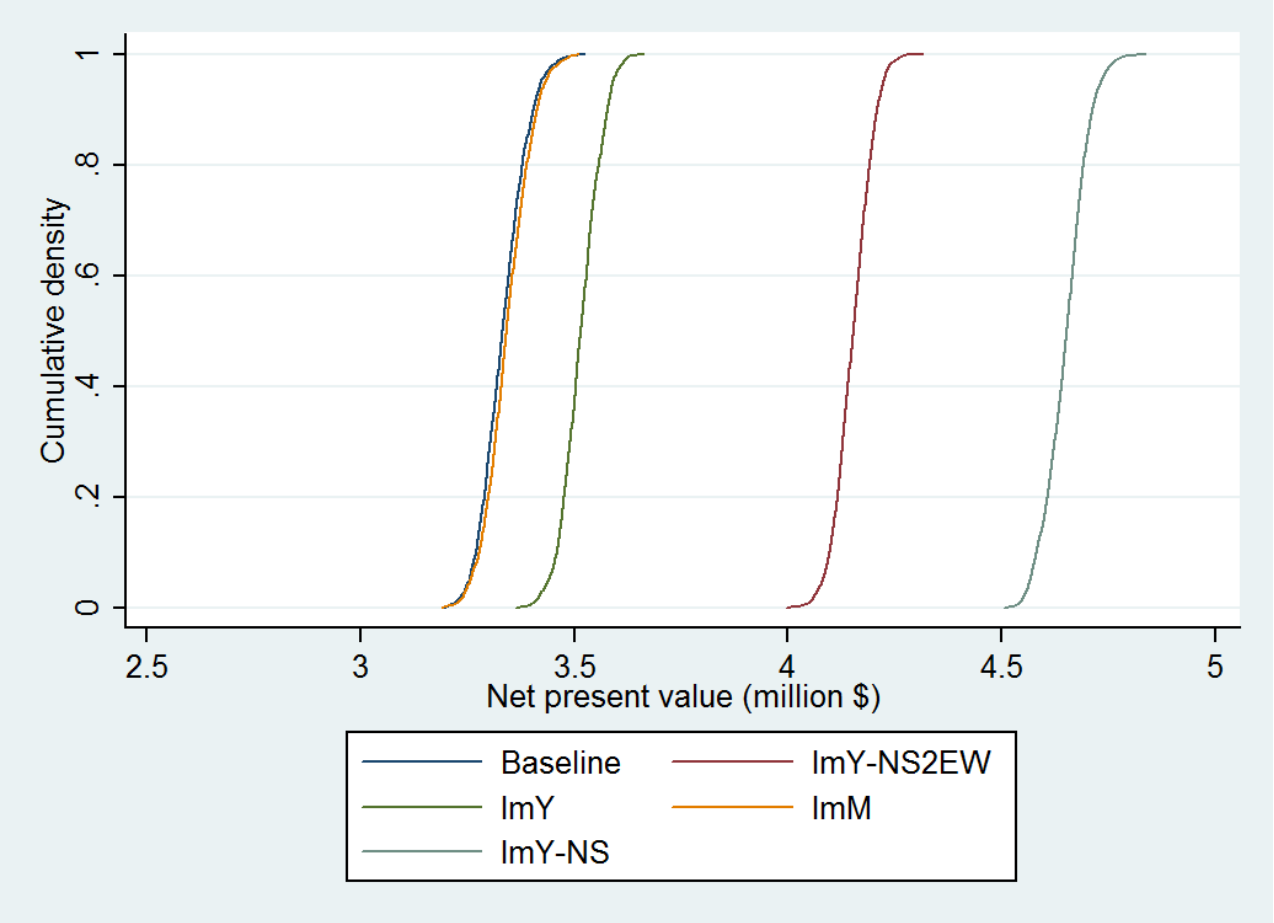

Endnotes

[1] Defined as the period in which insect vectors retain the virus and remain infective (Tsai et al. 2008).

[2] By comparing leaf reflectance measurements in the visible and near-infrared between healthy and infected leaves, the spectral reflectance technique can identify the health status of a plant.

[3] The represented vineyard dimensions are 350' x 650'with an area of 227,500 ft^2 or 5.22 acres. Vine and column spacing are 5 and 8 feet, respectively.

[4] Recall that the *Exposed* state is one where a vine is infected, nonsymptomatic, and noninfective

[5] An infective agent to the north (east) of a healthy agent transmits the disease with the same probability as the neighbor to the south (west) does.

[6] Although the authors report transmission rates as high as 60%, we limit the upper bound to 20% to account for the fact that transmission rates are lower in the field than in the laboratory.

[7] We do not include costs other than disease control costs because they are unchanged under the different disease control strategies.

[8] We exclude the strategy of roguing and replacing *Infective-high* and *Young* (I_hY) because this age-infection combination cannot be reached; it takes a vine more than 5 years to transition to the *Infective-high* state.

[9] In a First Order Stochastic Dominance test, for two cumulative distribution functions F_A and F_B, F_A dominates F_B if $F_A(y) \leq F_B(y), \forall\, y \in \mathbb{R}$

[10] Figure 2 shows one single realization of the disease diffusion process. Therefore, the realized half-life (read at the intersection of the red and dark green curves) does not correspond to the mean expected half-lives in table 3.

OTHER A.E.M. WORKING PAPERS

WP No	Title	Fee (if applicable)	Author(s)
2013-10	Labor Law violations in Chile		Kanbur, R., Ronconi, L. and L. Wedenoja
2013-09	The Evolution of Development Strategy as Balancing Market and Government Failure		Devarajan, S. and R. Kanbur
2013-08	Urbanization and Inequality in Asia		Kanbur, R. and J. Zhuang
2013-07	Poverty and Welfare Management on the Basis of Prospect Theory		Jäntti,M., Kanbur, R., Nyyssölä, M. and J. Pirttilä
2013-06	Can a Country be a Donor and a Recipient of Aid?		Kanbur, R.
2013-05	Estimating the Impact of Minimum Wages on Employment, Wages and Non-Wage Benefits: The Case of Agriculture in South Africa		Bhorat, H., Kanbur, R. and B. Stanwix
2013-04	The Impact of Sectoral Minimum Wage Laws on Employment, Wages, and Hours of Work in South Africa		Bhorat, H., Kanbur, R. and N. Mayet
2013-03	Exposure and Dialogue Programs in the Training of Development Analysts and Practitioners		Kanbur, R.
2013-02	Urbanization and (In)Formalization		Ghani, E. and R. Kanbur
2013-01	Social Protection: Consensus and Challenges		Kanbur, R.
2012-16	Economic and Nutritional Implications from Changes in U.S. Agricultural Promotion Efforts		Ho, S., Rickard, B. and J. Liaukonyte
2012-15	Welfare Effects of Biofuel Policies in the Presence of Fuel and Labor Taxes		Cooper, K. and D. Drabik
2012-14	Impact of the Fruit and Vegetable Planting Restriction on Crop Allocation in the United States		Balagtas, J., Krissoff, B., Lei, L. and B. Rickard
2012-13	The CORNELL-SEWA-WIEGO Exposure and Dialogue Programme: An Overview of the Process and Main Outcomes		Bali, N., Alter, M. and R. Kanbur

Paper copies are being replaced by electronic Portable Document Files (PDFs). To request PDFs of AEM publications, write to (be sure to include your e-mail address): Publications, Department of Applied Economics and Management, Warren Hall, Cornell University, Ithaca, NY 14853-7801. If a fee is indicated, please include a check or money order made payable to Cornell University for the amount of your purchase. Visit our Web site (*http://aem.cornell.edu/research/wp.htm)* for a more complete list of recent bulletins.